RSC Publishing Faraday Discussions

Toward SERS-based Point-of-Care approaches for Therapeutic Drug Monitoring: the case of Methotrexate.

Journal:	*Faraday Discussions*
Manuscript ID	FD-ART-11-2015-000173.R1
Article Type:	Paper
Date Submitted by the Author:	08-Jan-2016

Complete List of Authors:	Fornasaro, Stefano; University of Trieste, Department of Engineering and Architecture Dalla Marta, Silvia; University of Trieste, Department of Engineering and Architecture Rabusin, Marco; Institute for Maternal and Child Health (I.R.C.C.S.) Burlo Garofolo, UO Pediatric Hemato-Oncology Bonifacio, Alois; University of Trieste, Department of Engineering and Architecture Sergo, Valter; University of Trieste, Department of Engineering and Architecture

Faraday Discussions

PAPER

Toward SERS-based Point-of-Care approaches for Therapeutic Drug Monitoring: the case of Methotrexate.

Received 00th January 20xx,
Accepted 00th January 20xx

DOI: 10.1039/x0xx00000x

www.rsc.org/

Stefano Fornasaro[a†], Silvia Dalla Marta[a†], Marco Rabusin[b], Alois Bonifacio[a*] and Valter Sergo[a*]

To date, in spite of their toxicity, the plasmatic concentration of most chemotherapeutic drugs is difficult to monitor in oncological patients, because their quantitative determination is expensive and time consuming. This contribution reports a first attempt for the direct quantitative determination of a chemotherapeutic drug in human serum samples by means of Surface Enhanced Raman Spectroscopy (SERS). In this study, SERS substrates constituted by Au nanoparticles deposited on paper by a simple dipping method have been used for rapid (few minutes) analysis of diluted human serum spiked with different concentrations of methotrexate, MTX. The drug concentrations were chosen in a range designed to cover typical therapeutic plasmatic values (from nanomolar to millimolar) in oncological patients, and the pertinent calibration was obtained by Partial Least-Squares Regression (PLSR). Stability selection was employed to evaluate the capability of the PLSR model to accurately predict and extract spectral variations correlated to MTX concentration. Such a quantitative determination is crucial for a frequent, and hence adherent, Therapeutic Drug Monitoring, TDM, of chemiotherapic drugs, given their heavy side effects. Its low cost, rapid response and the possibility of obtaining spectra with simple and compact instruments, make SERS particularly apt for implementing an effective TDM. The promising results obtained in the analytical validation indicate which steps are to be taken on the way toward a clinical validation with real samples from oncological patients, for MTX as well as for other chemotherapeutic drugs.

Introduction

Therapeutic drug monitoring (TDM) is highly recommended in clinical settings to provide individualised patient treatment, optimising the efficacy of drugs with a narrow therapeutic window while minimising side effects[1].

Methotrexate (MTX, 2,4-diamine-*N*,10-methylpteroyl glutamic acid) is a folate antagonist included in anti-neoplastic and anti-rheumatic drugs. It is one of the most widely used anti-cancer agents, with indications and established protocols for a range of children's and adult cancers[2].

Unlike other chemotherapeutic agents, MTX is used in a wide variety of doses. Intermediate- and lower-dose MTX regimens (e.g., 20 mg/m^2) are used in maintenance chemotherapy and in the treatment of benign conditions such as psoriasis and rheumatoid arthritis[3], while much higher dose regimens (e.g., 1,000 mg/m^2 to 33,000 mg/m^2) via prolonged intravenous (IV) infusion are used for the treatment of some leukaemias and osteosarcomas[4]. The latter dose range is referred to as high-dose MTX (HDMTX).

The effective concentration range of MTX is limited to a relatively narrow therapeutic window, and dose adjustments during MTX therapy are routinely undertaken to address the high inter- and intra-patient variability in MTX pharmacokinetics[5]. Serum MTX concentrations can vary over 5 orders of magnitude (10 nM to 1 mM) from one patient to another using a single fixed dose and in the same patient during treatment[4]. Pharmacokinetic variability is generally greater in paediatric patients than in adults. For HDMTX therapy, it is usually desirable to reach initial serum concentrations between 10 to 100 µM, maintained for prolonged periods (12 to 36 hours), which must drop to less than 200 nM after 72 hours. The plasma MTX concentration at 48 hours after the start of HDMTX infusion should be <1 µM, as high-risk toxic, adverse effects are associated with concentrations >10 µM[6].

After HDMTX, monitoring MTX serum levels is thus crucial to reverse its side effects, such as myelosuppression, nephrotoxicity, hepatotoxicity, and death[6, 7].

MTX concentrations are routinely monitored, and rescue therapy is regulated on the basis of these measurements[8].

Several analytical methods have been reported for the TDM of MTX in biological fluids. Existing MTX assays include the Enzyme-Multiplied Immunoassay Technique (EMIT)[9], enzyme inhibition assays[10], the fluorescence polarisation immunoassay (FPIA)[11], radioimmunoassay[12], capillary zone electrophoresis[13], and liquid chromatography coupled with tandem mass spectrometry (HPLC-MS/MS)[14-18]. Very recently, an approach

[a.] *Department of Engineering and Architecture, University of Trieste, Trieste; Italy.*
[b.] *Institute for Maternal and Child Health (I.R.C.C.S.) Burlo Garofolo, UO Pediatric Hemato-Oncology, Trieste; Italy.*
† These authors contributed equally.
* Co-corresponding authors.

Electronic Supplementary Information (ESI) available: [details of any supplementary information available should be included here]. See DOI: 10.1039/x0xx00000x

for indirect MTX determination, based on SPR and having an excellent performance, was presented by Zhao et al[19].

HPLC-MS/MS is considered the reference standard technique for MTX analyses in biological fluids, though it is less commonly employed than immunoassays in clinical settings, since it is time consuming, expensive and requires specialised operators. Moreover, many of these routine methods lack precision, sensitivity, and a broad dynamic range; they still require protein precipitation or clean-up steps by passage through a pre-treatment column.

Because of its remarkable advantages such as rapidity, simplicity, relatively low costs, recent data on buffered aqueous MTX solutions suggested that the combination of Surface-Enhanced Raman Scattering (SERS) spectroscopy with multivariate statistical analysis could be a promising analytical tool for therapeutic drug monitoring of MTX[20, 21]. However, SERS approaches quantifying MTX directly in serum or other complex biofluids have not been reported yet.

In this work, we report promising preliminary results related to the application SERS combined with chemometrics for rapid MTX quantification in a complex, real-life sample such as diluted human serum. To obtain a predictive model as stable and as realistic as possible, a stability selection approach is employed to evaluate the capability of the model to accurately predict and extract spectral variations correlated to MTX concentration.

Experimental

Chemicals and reagents

All chemicals and solvents were of analytical reagent grade; they were purchased from Sigma-Aldrich (Milano, Italy) and used as received. Filter paper with 2 μm of pore size (qualitative filter paper, 410) was purchase from VWR International (Milano, Italy). Phosphate buffered saline solution (PBS) (pH 7.4) was prepared by dissolving a PBS tablet (Sigma-Aldrich) in Milli-Q water (200 mL). Serum samples used for method construction and validation were obtained from a healthy volunteer. All glassware used for gold nanoparticles (AuNPs) preparation was carefully cleaned with *aqua regia* and thoroughly rinsed with MilliQ water. For all cleaning procedures and preparation of solutions, MilliQ water was used.

SERS substrates preparation and characterisation

In-house built, solid SERS substrates were used in this study. Citrate-reduced gold nanoparticles (NP) were synthesised according to a protocol described by Turkevich et al., with slight modifications[22]. 10.6 mg of $NaAuCl_4$ were dissolved in 25 mL of Milli-Q water and heated to boiling. 750 μL of 1% sodium citrate were then rapidly added under vigorous magnetic stirring. The solution was kept boiling under stirring for 20 min. The AuNP colloidal solutions were stored in dark at room temperature (RT) and were stable at least for eight months[23]. During that time, neither aggregation was visible in the colloidal solutions, or any changing on their UV-visible spectra.

The colloids were characterised by UV-visible absorption spectroscopy after each preparation using a Lambda 20bio UV–Vis spectrometer (Perkin-Elmer, Monza, Italy). AuNPs feature a surface plasmon band at 540 ± 2 nm. The colloids were also characterised by Transmission Electron Microscope (TEM, Philips EM 208). Both UV–Vis extinction spectra and TEM images of AuNPs for different preparations can be found in the electronic supplementary material.

The solid SERS substrates were obtained using the dip-coating method[24-27], loading the NPs on the filter paper. A piece of 1 cm^2 was placed on the bottom of a cylindrical glass vial (total capacity of 10 mL) containing 3 mL of Au colloidal solution, to which sodium citrate was added up to a final concentration of 20 mM. The presence of the citrate leads to a colour change of the colloidal solution from red to grey-blue, indicating NP aggregation. The vials containing the filter paper were then stocked in dark at room temperature for one week; after this time, all the NPs were deposited on the vial bottom, covering the paper. The supernatant was extracted with a plastic syringe, paying attention not to touch or move the paper substrate. The substrates were then dried in the vials in air at room temperature and then stocked in Milli-Q water to avoid any loss of NP plasmonic activity. The repeatability of SERS measurements among different substrates has been checked using different analytes and the relative standard deviation over four different independent substrates was ≤15%.

Sample preparation and SERS measurements

MTX stock standard solution was prepared by dissolving 5.0 mg of MTX hydrate (>98% HPLC, Sigma-Aldrich) powder in 0.2 mL of 0.1 M sodium hydroxide and diluting to 10 mL in a volumetric flask with PBS solution. The MTX stock standard solution was then diluted to 100 μM in PBS, aliquoted for single use and stored at -20° C. Further dilutions were performed in 4% Bovine Serum Albumin (BSA)-PBS, a surrogate matrix frequently used to simulate plasma and serum, because its pH (7.4) and ionic strength (150 mM) are similar to those of the two biofluids. BSA was also added at a concentration of 40 g/L to simulate the protein content of serum. Such dilutions were performed at room temperature before analysis and in a dark room, to avoid MTX photodegradation. A set of eleven calibration standards was prepared in a concentration range of 0.1–20 μM for MTX. For the validation of the analytical method in a real-life matrix, calibration standards were prepared by spiking drug-free human serum with appropriate amounts of MTX stock solutions, keeping a constant 1:4, v/v ratio between serum and PBS. The final calibration range for MTX in diluted serum was 0.1–300 μM. The 5-fold dilution of serum standards upon spiking was chosen in analogy with the dilution procedures required for commercially available MTX immunoassays often used in clinical settings.

Small drops of 5 μL of both MTX solutions and spiked serum samples were deposited on the nanostructured paper substrates and allowed to dry (15 min).

Instrumentation

Normal Raman and SERS spectra were measured at room temperature (22 +- 0.5 °C) with an InVia Raman spectrometer (Renishaw plc, Wotton-under-Edge, UK) equipped with a Leica *DMLM* microscope (Leica Biosystems, Wetzlar, Germany) in a backscattering configuration. The excitation source was a high-power (360 mW) diode laser (Toptica Photonics AG, Germany) with an emission at 785 nm; the laser light was focused onto the sample via an x10 objective lens (NA 0.25). The spectrograph was equipped with a 1,200 lines/mm grating and a thermoelectrically cooled charge coupled device (CCD) camera. The calibration of the instrument was checked prior to each measurement using the 520 cm^{-1} band of a silicon reference sample.

To facilitate handling, each 8 mm × 8 mm paper substrate was adhered to a standard microscope slide (25 mm × 75 mm) immobilized onto the microscope stage.

SERS spectra were recorded over a wavenumber range of 300–1900 cm^{-1}, using the "extended" acquisition mode of the InVia Raman microscope. All spectra were recorded using an accumulation of three scans (10 s exposure each, for a total of 30 s) at 6 random locations on the substrate surface, with 18 mW of laser power delivered to the sample. Instrument settings were optimised to maximise signal and minimise saturation or sample degradation arising from laser stimulation. In particular, the laser power density at the sample was decreased upon increasing the diameter of the laser spot using the "defocusing" option (90%) of the InVia Raman microscope. The system was controlled and data were collected by WiRE 3.2 software (Renishaw).

Data pre-processing

Special attention was paid to spectral data pre-processing [e.g., offset-Baseline Correction (BC), Area Normalisation (AN), and Multiplicative Scatter Correction (MSC)] for the purpose of outlier rejection, dimensionality reduction, and improvement in the robustness and accuracy of subsequent calibration models. First, the spectral region between 350 and 1700 cm^{-1} was selected for analysis. Then, the pre-processing workflow consisted of five steps: (i) removal of cosmic rays; (ii) BC; (iii) smoothing interpolation to increase the signal to noise ratio and to reduce the number of data points per spectrum (reduction of the dimensionality of the data); (iv) AN or MSC; and (v) outlier detection/removal by Principal Component Analysis (PCA).

All spectra pre-processing was performed within the R software environment for statistical computing and graphics[28]. In particular, data import and export, pre-processing, and visualisation were performed with the hyperSpec package[29] for R; for BC, a fourth-order polynomial baseline was fit automatically to the whole spectral range and subtracted from each spectrum of the dataset using the *modpolyfit* function from the package baseline[30]; peak picking was performed using *detectPeaks* from the MALDIquant[31] package. Anomalous spectra were automatically discarded by the *pcout* function from the package mvoutlier[32]. After the elimination of the outliers, the procedure was continually repeated until no more outliers were identified, in a self-consistent process. Eventually, a total of 6 spectra (over 99) were discarded as outliers (Figures S4-5).

Data analysis

All data analysis was performed within the R software environment for statistical computing and graphics[28] building on the pls[33] and glmnet[34] packages.

Partial Least Square Regression

For multivariate calibration, we employed Partial Least Squares Regression (PLSR) models to establish a relationship between the MTX levels and spectral data[35]. PLSR is a multivariate statistical method widely used in spectroscopy that aims at building a model that relates the variations of the spectral data (X matrix) to a series of relevant targets (Y matrix) according to the linear equation Y = XB+E, where B is a matrix of regression coefficients and E is a matrix of residuals. PLSR reduces the data to a small number of latent variables, maximising the covariance between the spectral data and the property to be modelled (in this case, MTX concentration).

The Repeated Double Cross-Validation (RDCV) strategy[36] was adopted for the optimisation of the complexity of PLSR models and to independently estimate the model performance for test set objects that have not been used in any step of model creation or optimisation. The optimum number of latent variables was selected by RDCV with 100 repetitions, applying the *one-standard-error-rule*[37]. Model performance was judged on the basis of the Root Mean Square Error of Prediction (RMSEP).

Stability selection

Stability selection was exploited to assess the variability of the model coefficients, selecting those that remain consistently important after repeated subsampling of the data. Our settings were as follows: (i), some uninformative variables were automatically eliminated by Elastic Net (EN) estimation (α=0.5) to subgroup the candidate variables and obtain a parsimonious model while retaining as much relevant information as possible. This procedure presents significant advantages for model interpretation. According to a strategy proposed for biomarker identification[38], the perturbation of the data was obtained (i) by leaving out 30% of the samples and considering only half of the variables at each iteration; (ii), the recursive PLSR calibration models were then built based on the strongly correlated variable obtained by the EN. Several PLSR models were calculated for prediction of the known concentration of MTX from the spectral data, varying the pre-processing methods and EN setup.

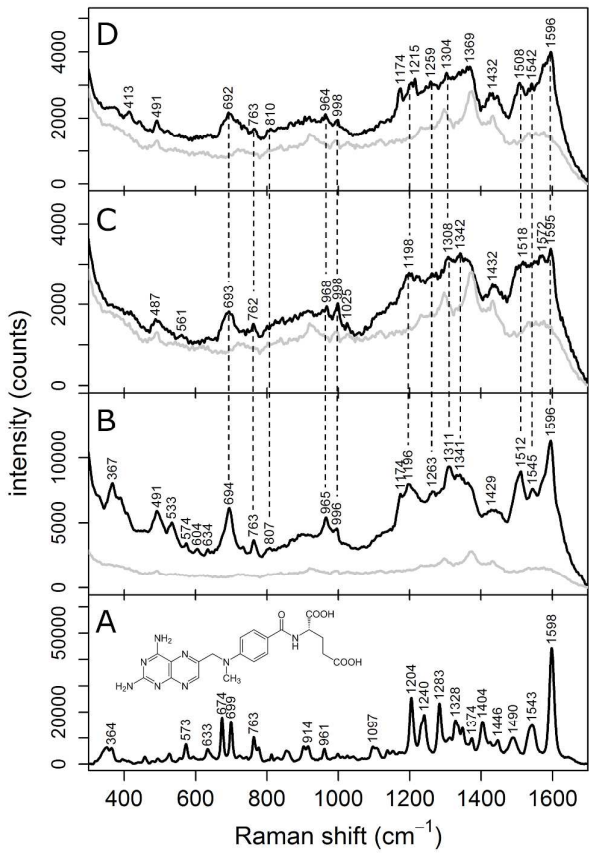

Figure 1 (**A**) Normal Raman spectrum of MTX powder; (**B**) SERS spectrum of MTX 10 µM in PBS, (**C**) SERS spectrum of MTX in 4% BSA-PBS, and (**D**) SERS spectrum of MTX diluted in human serum (1:4, v/v). The background signal of the substrate (grey line) is reported for comparison together with SERS spectra. The chemical structure of MTX is reported for reference in (A). All spectra were collected using an excitation at 785 nm.

Results and discussion

Comparison of SERS and Raman spectra of MTX samples

Figure 1 shows the normal Raman spectrum of the MTX powder, along with the SERS spectra of 10 µM MTX in aqueous solutions and diluted human serum. For this preliminary study, we used diluted human serum instead of undiluted serum. This choice was made to limit the overall amount of biofluid needed, as well as because diluted samples were easier to work with than undiluted ones, which are rather viscous and tend to foam upon mixing. For these reasons, diluted serum is routinely used in analytical and clinical settings[39]. Moreover, we observed that dilution does not significantly influence SERS spectra as acquired using our substrates (Figure S3A, B).

The characteristic Raman bands of MTX were consistent with those previously reported for this drug[20, 40-42]. Compared to the normal Raman, SERS bands of the MTX solution in PBS had slightly different positions, relative intensities and widths, as often observed for SERS spectra. Such differences are explained by invoking surface selection rules (for changes in relative intensities) and direct interaction of some molecule moieties with the metal surface (for shifts of band frequencies). Moreover, an underlying background due to traces of amorphous carbon in SERS spectra can be inferred from a generally increased intensity around 1360 and 1560 cm^{-1}, due to two broad bands (also called "cathedral bands") originating from stretching modes of sp^2 carbons[43-46]. Such bands are often observed when employing solid SERS substrates, because of a minimal photodegradation as a consequence of laser illumination. However, amorphous carbon has a very high Raman cross-section, so that even small quantities will yield a detectable background. In our measurements, the presence of amorphous carbon is kept to a minimum by ensuring a low laser power density (see Methods), and thus it is not interfering with MTX detection. Also worth mentioning is the definite background signal given by the SERS substrates themselves, reported in light grey in figure 1 along with SERS spectra. This background is largely due to the SERS signal of citrate ions[47], originally present as stabilizing adsorbates on the surface of colloidal Au NPs used to prepare the SERS substrates. Being constant, this substrate background can be assumed not to interfere with MTX detection.

Despite some differences, several bands in SERS spectra were observed at Raman shifts very close to those of the normal Raman spectrum of MTX, so that in some cases a direct correlation between Raman and SERS modes is straightforward. This is the case for the normal Raman bands at 699, 763, 961, 1204 and 1598 cm^{-1}, whose correspondence to their SERS counterparts is evident, for all three SERS spectra reported. A detailed and complete assignment of the SERS bands of MTX to vibrational modes, as well as a detailed description of the MTX-metal interaction, is out of the scope of this paper, and it would require carrying out an *ab-initio* computational study at the level of Density Functional Theory (DFT). The reader interested in a tentative assignment of the SERS bands is referred to[40-42]. As this paper is concerned with MTX detection in diluted serum, it is noteworthy that the SERS bands appearing at 491, 694, 965, 996, 1512 and 1596 cm^{-1} in the spectrum of the MTX in PBS solution (B), can be easily retrieved in both SERS spectra of MTX in presence of albumin (C) and in diluted serum (D). In other words, MTX can be detected with SERS even in a complex medium such as diluted serum. It is interesting to note that the presence of albumin appears to affect the MTX SERS signal, both in terms of absolute intensity [(C) spectrum is less intense than (B)] as well as in terms of slight band shifts. This is not unexpected, since MTX is known to bind to albumin, so that only about 50% of the drug is found as "free" molecule in serum, while the other 50% is tightly bound to the protein. Indeed, the absolute intensity of the MTX in presence of albumin, as well as that of MTX in serum, is approximately 40% of the absolute intensity counts observed for the drug in PBS, i.e. without the protein. Considering that the enhancement due to SERS dramatically decrease with the distance from the metal surface, so that only MTX molecules directly adsorbed onto the SERS substrate will significantly contribute to the signal, this decrease in SERS

Table 1 Details of several models for prediction of MTX levels in surrogate matrix (4% BSA-PBS) and diluted human serum (HS), using different pre-processing methods. **BC** offset-Baseline Correction; **AN** Area Normalization; **MSC** Multiplicative Scatter Correction; **N** number of wavelengths in the model; **RMSEP** units are in µM. **LVs**, Latent Variables in the double cross-validated models.

		4% BSA-PBS (n=59)				**HS** (n=93)			
Pre-processing	**Model**	**N**	**#LVs**	**R^2**	**RMSEP**	**N**	**#LVs**	**R^2**	**RMSEP**
None	PLS	2701	4	0.939	1.49	2701	3	0.524	37.21
	EN-PLS	154	2	0.9474	1.35	138	2	0.5568	40.41
BC	PLS	2701	3	0.953	1.28	2701	2	0.5206	36.95
	EN-PLS	94	2	0.9584	1.08	145	2	0.6387	31.57
MSC	PLS	2701	3	0.9342	1.41	2701	1	0.5187	37.3
	EN-PLS	89	2	0.9428	1.39	110	1	0.6416	32.16
AN	PLS	2701	3	0.9475	1.25	2701	2	0.5277	36.74
	EN-PLS	591	2	0.957	1.15	1195	2	0.5492	34.93
BC + AN	PLS	2701	2	0.9575	1.18	2701	1	0.521	37.5
	EN-PLS	243	1	0.9613	1.19	597	1	0.6181	33.76
BC+MSC	PLS	2701	2	0.9596	1.11	2701	1	0.5187	37.38
	EN-PLS	88	1	0.9555	1.19	126	1	0.661	32.51

intensity can be readily explained assuming that albumin-bound MTX are prevented from adsorbing onto the metal, while free MTX must compete for the surface with albumins themselves.

In the case of human serum, the complexity and variability in the matrix composition pose an even harder challenge for calibration and analysis. Serum has several thousands of components, with more than 4000 metabolites[48], some of which have a high affinity for gold surfaces, as proven by the intense SERS signal given by serum when using Au metal colloids[49]. To be observed, MTX must compete with all the serum constituents for adsorption. However, serum MTX concentration can be high, relatively to most metabolites, and, while the presence of albumin appears to affect the overall intensity, MTX affinity for Au appears competitive enough to keep its SERS signal well detectable. This affinity can be partially explained by looking at its chemical structure: heterocyclic nitrogens, carboxylate groups as well as primary amine groups present in MTX are capable of a strong interaction with gold[50]. Such strong MTX-Au interaction is responsible of the intense MTX SERS signal, and it makes possible the detection of this drug even in diluted serum.

Indeed, other authors have previously reported quantification of aqueous solutions of MTX based on SERS spectra. Hidi et al. used the SERS band around 965 cm^{-1} for quantitative detection by relating the Lorentz fitted peak area directly to the MTX concentration in KOH solution[20]. However, because of the increased complexity and lower S/N ratio of our SERS spectra obtained in presence of albumin or in diluted serum, the correlation of any individual band area with the MTX concentration was rather low and an univariate regression approach resulted in poor prediction of the MTX content (Figure S6). Nonetheless, the spectral signature of MTX is specific, and many Raman shifts (to be considered as variables for chemometrics purposes) were correlated to the MTX concentration. These features made possible selective measurements of MTX by combining spectral information across a wide range of wavenumbers. As stated, in this study, we focused on the wide region between 350 and 1700 cm^{-1} to build a multivariate calibration model that incorporates much of the available spectral information.

Multivariate calibration

Assessment of the analytical performances

Multivariate calibration aims to establish a model that relates the variations of the spectral data to a series of known concentrations. PLSR modelling is particularly suited in multivariate calibration models for strongly correlated and multi-collinear spectral data, where the number of variables exceeds the sample size[51]. PLSR iteratively maximises the covariance between the spectral matrix and the reference data and produces highly interpretable Latent Variables (LVs) that describe diminishing quantities of spectral variance in the context of the reference data. The construction of an entirely accurate PLSR model required the careful selection of a number of latent variables (LVs). PLSR models were calculated using spectra with and without pre-processing with the application of different techniques. An overview of their influence on the model's ability to predict the MTX concentration from the SERS spectra is reported in Table 1. In general, the best models have as few components as possible and provide the lowest prediction error for the number of components used. Interestingly, pre-processing does not appear to dramatically affect models performance in terms of RMSEP.

Quantification of MTX levels in surrogate matrix

The EN-selected model shown in Figure 2 provided an MTX concentration prediction of R^2=0.9584, RMSEP=1.08. Only two LVs were needed for the model; this number is reasonable given the number of solution components and the spectral variance resulting from variations in the background spectra.

Stability Selection

The EN-selected model for MTX in the surrogate matrix (Figure 2A) achieved the lowest error using only 94 wavelengths and 2

LV. It should be noted that the wavelength selection was not based on an explicit minimisation of prediction error, the criterion used in virtually all other variable selection methods. In fact, in cases with a low number of samples, this approach is usually not very reliable, increasing the risk of overfitting.

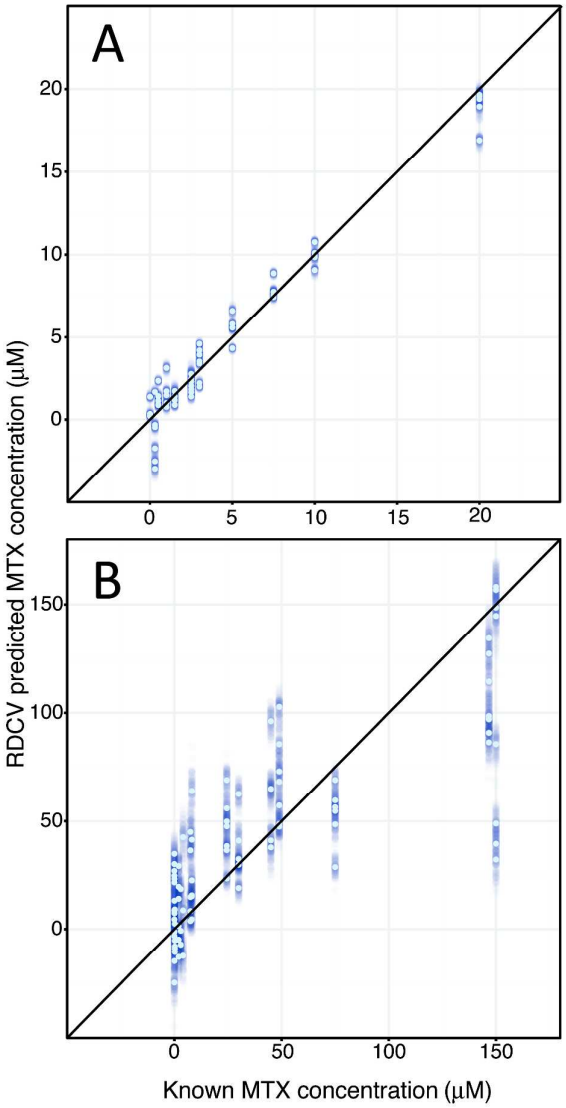

Figure 2 Diagnostic plots from Repeated Double Cross Validation (RDCV) for SERS data collected in (A) 4% BSA-PBS, and (B) diluted human serum. The results from the 100 repetitions in RDCV are reported in blue (for 4% BSA-PBS they are very close together and therefore mostly hidden); the means of 91 predictions are reported in light blue.

Stability selection, in contrast, using an approach inspired by random forests[52], does not explicitly seek to minimise prediction error but only identifies the variables that are consistently important. The central idea is that real differences should be present consistently in the dataset and therefore should be found even under perturbation of the data by subsampling[38, 53]. The EN approach is based on a relatively new version of penalised least squares. It employs a shrinkage with a penalty that is a compromise between the Ridge regression penalty (α=0) and the Least Absolute Shrinkage and Selection Operator (LASSO) regression penalty (α=1)[54]. Stability selection made the data more succinct and provided a good interpretation of the model, revealing an explicit relationship between the MTX levels and the spectral variables. As the Regression Coefficients (RC) are descriptors of the spectral features that were used to build the model, we also aimed at assessing the accuracy with which the algorithm can faithfully use the known spectral profiles of MTX. In Figure 3A, a direct comparison between the RC of the PLSR model and a MTX SERS spectrum is shown, highlighting the frequency with which different Raman shifts are chosen by the EN algorithm. This figure allows the data analyst to check that the variation of MTX levels, rather than the spectral variance of the matrix, plays a relevant role in the PLSR model construction. If so, both EN-selected Raman shifts (coloured in red in Figure 3) and high values for RC should coincide as much as possible with SERS bands of MTX. This is clearly the case for the EN-PLS model for MTX in surrogate matrix (Figure 3A).

Quantification of MTX in human serum

The PLSR modelling process was repeated for the calibration of MTX concentration in diluted human serum, using the stability selection and pre-processing steps proposed in the Assessment of Analytical Performance section. Among blood sample types (whole blood, plasma, and serum), serum was selected in our study because i) it retains most substances present in blood while not being subject to blood cell interference, ii) it does not contain anticoagulants which might interfere with the spectroscopic signal due to the drug[49]. Actual measurements were performed on diluted serum samples, as detailed in the experimental section, for the reasons previously mentioned.

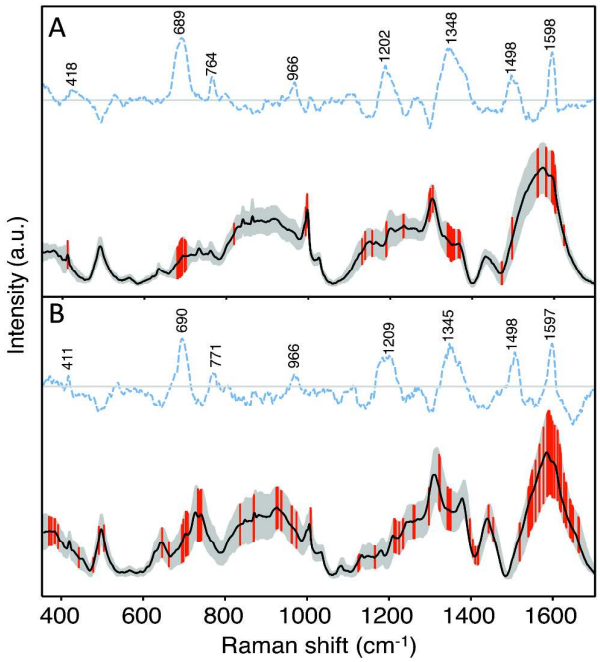

Figure 3 Average spectra (black line) overlaid with EN selected. The blue dotted line shows a plot of the regression coefficient (RC) following PLSR. The RC has been offset for clarity.

The EN-selected multivariate calibration achieved the lowest error, using only 120 wavelengths and 1 LV, yielding an RMSEP of 31.78 μM, with an R^2 of 0.6387.

Based on these values, it can be seen that the model produces a poorer prediction than the one built for the surrogate matrix. This is somewhat expected, considering the increased complexity of real serum with comparison to a buffered albumin solution. Considering that in this preliminary study we used serum samples from a single donor, inter-individual variations in serum composition can be ruled-out as a reason for the increased dispersion observed for data obtained from diluted serum with respect to those from buffered albumin solution. As serum itself does not yield intense SERS bands (see Figure S3A, B), intra-individual changes in composition, as well as the usual experimental errors involved in sample preparation and spiking, might be indirect sources of variation in SERS data by modulating the interaction of MTX with the metal surface. Inspection of the MTX RC in Figure 3B shows that the bands of the MTX SERS spectrum are faithfully reproduced and dominate the MTX RC. The correlation between EN-selected Raman shifts and MTX SERS bands is less straightforward. The different distribution of the EN-selected Raman shifts in the serum spectra is justified by the complexity of the biological matrix; the occurrence of so many components with the ensuing spectral complexity clearly affects the stability selection[54].

Relevant implications

MTX requires careful diagnostic monitoring because of severe host side effects. Its concentration in plasma or serum is commonly screened with various techniques, and the dosage is regulated to the optimal therapeutic region by taking into account the patient characteristics[5]. Although there is an urgent demand for a faster and cheaper alternative to HPLC-MS/MS MTX assays, a sensitive and reliable SERS methodology for TDM of MTX is still a challenge. To our knowledge, however, SERS-based MTX quantification, or even detection, in diluted or undiluted human serum has not yet been reported.

The methodology presented in this work clearly demonstrates that SERS in combination with multivariate data analysis has the capability for the quantitative detection of MTX in human serum. Furthermore, multivariate calibration in conjunction with stability selection, as demonstrated here, produces less complex and more accurate models because of the targeted inclusion of frequency bands specific to the analyte in question. As expected, in a comparison between the calibration and prediction errors listed in Table 1, 4% BSA-PBS spectra usually outperform the analogous models generated from diluted serum spectra. Scatter is noticeably greater, leading to a large standard deviation in response.

Quantification using SERS has been since long recognized as a challenging task[55], mainly because of poor repeatability and reproducibility, two flaws which were often reported for colloidal SERS substrates. The use of standard additions[56] or internal standards[57-59] has been proposed by some authors to tackle these problems, but it is evident that the availability of repeatable and reproducible inexpensive SERS substrates would be a main solution. The paper-based SERS substrates used in this study proved to be capable of quantification, as clearly shown in the case of MTX in a surrogate matrix.

When the method is applied to diluted serum measurements, the observed prediction error for MTX (31.78 μg/g) is still significantly higher than what is observed for established reference HPLC-MS/MS methods[16], and thus an increase in precision of the SERS method is still necessary. Considering the difficulty of achieving quantification in a complex matrix using SERS, however, results reported in this study still represent a significant step forward.

Moreover, it is important to note that the SERS substrate used in this study was not specifically adapted to target MTX. A gold surface might be functionalised to promote a selective adsorption of the analyte of interest while maintaining the integrity and activity of the compound[60], at the same time preventing the competition for the adsorption sites with the other serum components. Various strategies can be suggested to increase the affinity of the substrates for the drugs, including molecular recognition approaches such as MIP (molecularly imprinted polymers)[17] and artificial peptides. Such approaches are currently under investigation by our group, so that in the future the accuracy and precision of MTX quantification can be further improved. Furthermore, a functionalization of the SERS substrates would broaden the applicability of our SERS/EN-PLSR method, paving the way to its use with those chemotherapeutic drugs lacking the strong affinity for Au surfaces shown by MTX.

Conclusions

The present work clearly shows that, by using repeatable substrates and an adequate data analysis, the quantification of drugs by SERS in complex biological matrices, diluted serum in our case, is possible.

Also, our data provide an estimate of the difference in the quantification performance to be expected in real serum with respect to model solutions. The increased chemical complexity of serum with respect to model solutions, translates in a decrease of one order of magnitude in the precision (RSMEP) of the drug quantification.

Acknowledgements

SF acknowledges support from IRCCS Burlo Garofolo. This article is based upon work from COST Action BM1401 Raman-based applications for clinical diagnostics (Raman4Clinics), supported by COST (European Cooperation in Science and Technology

Bibliographic references

1. E. Llorente Fernandez, L. Pares, I. Ajuria, F. Bandres, B. Castanyer, F. Campos, C. Farre, L. Pou, J. M. Queralto and J. To-Figueras, *Clinical chemistry and*

laboratory medicine : CCLM / FESCC, 2010, **48**, 437-446.
2. K. Barnhart, C. Coutifaris and M. Esposito, *Expert opinion on pharmacotherapy*, 2001, **2**, 409-417.
3. J. Jolivet, K. H. Cowan, G. A. Curt, N. J. Clendeninn and B. A. Chabner, *The New England journal of medicine*, 1983, **309**, 1094-1104.
4. N. Graf, K. Winkler, M. Betlemovic, N. Fuchs and U. Bode, *Journal of clinical oncology : official journal of the American Society of Clinical Oncology*, 1994, **12**, 1443-1451.
5. H. Seidel, A. Andersen, J. Terje Kvaløy, R. Nygaard, P. J. Moe, G. Jacobsen, B. Lindqvist and L. Slørdal, *Leukemia Research*, 2000, **24**, 193-199.
6. Y. A. A. R. Ahmed and Y. Hasan, *J Cancer Sci Ther*, 2013, **5**, 106-112.
7. B. C. Widemann and P. C. Adamson, *Oncologist*, 2006, **11**, 694-703.
8. A. Paci, G. Veal, C. Bardin, D. Leveque, N. Widmer, J. Beijnen, A. Astier and E. Chatelut, *European journal of cancer*, 2014, **50**, 2010-2019.
9. M. P. Borgman, M. F. Hiemer, A. R. Molinelli, J. C. Ritchie and S. A. Jortani, *Ther Drug Monit*, 2012, **34**, 193-197.
10. B. C. Widemann, F. M. Balis and P. C. Adamson, *Clinical chemistry*, 1999, **45**, 223-228.
11. M. A. Pesce and S. H. Bodourian, *Ther Drug Monit*, 1986, **8**, 115-121.
12. J. J. Langone, *Methods in enzymology*, 1982, **84**, 409-422.
13. C. Y. Kuo, H. L. Wu, H. S. Kou, S. S. Chiou, D. C. Wu and S. M. Wu, *Journal of chromatography. A*, 2003, **1014**, 93-101.
14. Y.-D. Li, Y. Li, N.-S. Liang, F. Yang and Z.-P. Kuang, *J Chromatogr B Analyt Technol Biomed Life Sci*, 2015, **1002**, 107-112.
15. R. C. Schofield, L. V. Ramanathan, K. Murata, M. Grace, M. Fleisher, M. S. Pessin and D. C. Carlow, *J Chromatogr B Analyt Technol Biomed Life Sci*, 2015, **1002**, 169-175.
16. E. Sonemoto, N. Kono, R. Ikeda, M. Wada, Y. Ueki and K. Nakashima, *Biomed Chromatogr*, 2012, **26**, 1297-1300.
17. S. Chen and Z. Zhang, *Spectrochim Acta A Mol Biomol Spectrosc*, 2008, **70**, 36-41.
18. G. Rule, M. Chapple and J. Henion, *Anal Chem*, 2001, **73**, 439-443.
19. S. S. Zhao, N. Bukar, J. L. Toulouse, D. Pelechacz, R. Robitaille, J. N. Pelletier and J.-F. Masson, *Biosens Bioelectron*, 2015, **64**, 664-670.
20. I. J. Hidi, A. Mühlig, M. Jahn, F. Liebold, D. Cialla, K. Weber and J. Popp, *Analytical Methods*, 2014, **6**, 3943.
21. J. Yang, M. M.-C. Cheng, X. Tan and W.-C. Shih, *Biomedical Microdevices*, 2014, **16**, 673-679.
22. J. Turkevich, P. C. Stevenson and J. Hillier, *Discuss. Faraday Soc.*, 1951, **11**, 55-75.
23. J. Kimling, M. Maier, B. Okenve, V. Kotaidis, H. Ballot and A. Plech, *The journal of physical chemistry. B*, 2006, **110**, 15700-15707.
24. L. Polavarapu and L. M. Liz-Marzan, *Phys Chem Chem Phys*, 2013, **15**, 5288-5300.
25. C. H. Lee, L. Tian and S. Singamaneni, *ACS applied materials & interfaces*, 2010, **2**, 3429-3435.
26. C. H. Lee, M. E. Hankus, L. Tian, P. M. Pellegrino and S. Singamaneni, *Anal Chem*, 2011, **83**, 8953-8958.
27. Y. H. Ngo, D. Li, G. P. Simon and G. Garnier, *Langmuir : the ACS journal of surfaces and colloids*, 2012, **28**, 8782-8790.
28. The R Core Team, *Journal*, 2014.
29. C. Beleites and V. Sergo, *R package version 0.98-20140523*, 2014.
30. K. Hovde Liland and r.-H. M. BjÃ, *Journal*, 2015.
31. S. Gibb and K. Strimmer, *Bioinformatics*, 2012, **28**, 2270-2271.
32. P. Filzmoser and M. Gschwandtner, *Journal*, 2015.
33. B. H. Mevik and R. Wehrens, *Journal of Statistical Software*, 2007, **18**.
34. J. Friedman and T. Hastie, *glmnet: Lasso and elastic-net regularized generalized linear models*, R package …, 2009.
35. K. Varmuza and P. Filzmoser, *Introduction to multivariate statistical analysis in chemometrics*, 2009.
36. P. Filzmoser, B. Liebmann and K. Varmuza, *Journal of Chemometrics*, 2009, **23**, 160-171.
37. T. Hastie, R. Tibshirani and J. H. Friedman, *The elements of statistical learning: data mining, inference, and prediction*, Springer, New York, NY, 2nd edn., 2013.
38. R. Wehrens, P. Franceschi, U. Vrhovsek and F. Mattivi, *Anal Chim Acta*, 2011, **705**, 15-23.
39. Q. A. Xu and T. L. Madden, *Analytical methods for therapeutic drug monitoring and toxicology*, Wiley-Blackwell, Oxford, 2011.
40. Y. Ozaki, R. W. King and P. R. Carey, *Biochemistry*, 1981, **20**, 3219-3225.
41. G. Seng, J. Bolard and L. Chinsky, *Journal of Raman …*, 1982.
42. D. D. Saperstein, A. J. Rein and M. Poe, *Journal of the American …*, 1978.
43. R. A. Alvarez-Puebla, *The journal of physical chemistry letters*, 2012, **3**, 857-866.
44. J. L. Castro, J. C. Otero and J. I. Marcos, *Journal of Raman Spectroscopy*, 1997, **28**, 765-769.
45. S. Sánchez-Cortés and J. V. García-Ramos, *Journal of Raman Spectroscopy*, 1998, **29**, 365-371.
46. J. S. Suh, M. Moskovits and J. Shakhesemampour, *The Journal of Physical Chemistry*, 1993, **97**, 1678-1683.
47. C. H. Munro, W. E. Smith, M. Garner, J. Clarkson and P. C. White, *Langmuir : the ACS journal of surfaces and colloids*, 1995, **11**, 3712-3720.
48. N. Psychogios, D. D. Hau, J. Peng, A. C. Guo, R. Mandal, S. Bouatra, I. Sinelnikov, R. Krishnamurthy, R.

Eisner, B. Gautam, N. Young, J. Xia, C. Knox, E. Dong, P. Huang, Z. Hollander, T. L. Pedersen, S. R. Smith, F. Bamforth, R. Greiner, B. McManus, J. W. Newman, T. Goodfriend and D. S. Wishart, *PLoS ONE*, 2011, **6**, e16957.

49. A. Bonifacio, S. D. Marta, R. Spizzo, S. Cervo, A. Steffan, A. Colombatti and V. Sergo, *Analytical and Bioanalytical Chemistry*, 2014, **406**, 2355-2365.
50. L. Guerrini, Z. Jurasekova, C. Domingo, M. Pérez-Méndez, P. Leyton, M. Campos-Vallette, J. V. Garcia-Ramos and S. Sanchez-Cortes, *Plasmonics*, 2007, **2**, 147-156.
51. M. E. Keating, H. Nawaz, F. Bonnier and H. J. Byrne, *The Analyst*, 2015, **140**, 2482-2492.
52. L. Breiman, *Machine learning*, 2001.
53. N. Meinshausen and P. Bühlmann, *J. R. Statist. Soc. B*, 2010, **72**, 417-473.
54. G.-H. Fu, Q.-S. Xu, H.-D. Li, D.-S. Cao and Y.-Z. Liang, *Appl Spectrosc*, 2011, **65**, 402-408.
55. M. Sackmann and A. Materny, *Journal of Raman Spectroscopy*, 2006, **37**, 305-310.
56. E. Kammer, K. Olschewski, S. Stockel, P. Rosch, K. Weber, D. Cialla-May, T. Bocklitz and J. Popp, *Anal Bioanal Chem*, 2015, **407**, 8925-8929.
57. W. Shen, X. Lin, C. Jiang, C. Li, H. Lin, J. Huang, S. Wang, G. Liu, X. Yan, Q. Zhong and B. Ren, *Angewandte Chemie*, 2015, **54**, 7308-7312.
58. Y. Zhou, R. Ding, P. Joshi and P. Zhang, *Anal Chim Acta*, 2015, **874**, 49-53.
59. A. M. Fales and T. Vo-Dinh, *Journal of Materials Chemistry C*, 2015, **3**, 7319-7324.
60. R. A. Sperling and W. J. Parak, *Philosophical Transactions of the Royal Society A: Mathematical, Physical and Engineering Sciences*, 2010, **368**, 1333-1383.